Classification
Physics Abstracts
61.30 — 64.70M

X-ray reflectivity of classical smectic-A liquid crystals

E. F. Gramsbergen ([1]) and W. H. de Jeu ([2])

([1]) Solid State Physics Laboratory, Melkweg 1, 9751 EP Groningen, The Netherlands
([2]) FOM-Institute for Atomic and Molecular Physics, Kruislaan 407, 1098 SJ Amsterdam, and Open University P.O. Box 2960, 6401 DL Heerten, The Netherlands

(Reçu le 26 août 1987, accepté le 23 octobre 1987)

Résumé. — On étudie la stratification en couches d'un cristal liquide polaire NCS lorsqu'il passe d'une phase nématique à une structure smectique A classique en monocouches ; la méthode utilisée est l'étude de la surface du matériau par mesure de la réflectivité des rayons X. On observe la formation de monocouches à la surface du cristal liquide, sans qu'il y ait rupture de la symétrie haut-bas. Ce comportement est contraire à celui des composés polaires substitués CN qui forment des bicouches à la surface et une phase smectique A1 dans la profondeur du matériau. On discute les conséquences de ces résultats pour les modèles moléculaires des phases smectiques A.

Abstract. — Using X-ray reflectivity smectic layering is investigated on both sides of a classical monolayer smectic-A to nematic phase transition in a polar NCS substituted compound. At the surface, only monolayering is observed ; there is no breaking of up-down symmetry. This contrasts with the situation of a smectic-A1 phase in a polar CN substituted compound, where bilayering occurs at the surface. Consequences for molecular models of smectic-A phases are discussed.

1. Introduction.

Smectic-A (S_A) liquid crystal mesophases are layered phases in which elongated molecules are aligned along the layer normal **n** with liquid-like in-plane order. In the classical picture of the S_A phase any molecular asymmetry is nullified by a random up-down order on the scale of a few molecules. Other possibilities arise when the intermolecular forces connected with the molecular asymmetry are strong ; in practice this is the case for terminal dipoles like CN or NO_2. Then a variety of S_A phases is possible due to the additional dipolar ordering of the molecules. Detailed descriptions of the monolayer S_{A1}, bilayer S_{A2} and partially bilayer $S_{\tilde{A}}$ and S_{Ad} phases have been given elsewhere [1, 2]. In phase diagrams, these phases often appear in the succession S_{A1}-$S_{\tilde{A}}$-S_{A2} or S_{Ad}-S_{A2} as the temperature is lowered. In this paper, we reserve the name « classical S_A» for S_A phases in which the up-down ordering in the layers is completely random ; it is distinguished from the S_{A1} phase which has antiferroelectric short-range order. Arguments for this distinction will be given in the discussion.

In an earlier experiment, the surface of an S_{A1} liquid crystal was found to break the up-down symmetry, thereby inducing a few S_{A2}-like bilayers [3, 4]. Other cases reported in the literature involve either S_A phases without polar endgroups or S_{Ad} phases in which the molecules are, to a great extent, coupled into dimers that are naturally up-down symmetric. In both cases, it is not surprising that no additional bilayering occurs at the surface. One possibility not yet investigated is that of a classical S_A phase of polar molecules. The objective of this paper is to test whether the surface field is strong enough here to polarize the first molecular layer at the surface so that bilayers can develop as in the S_{A1} phase. We therefore choose a compound with an NCS endgroup, which has a considerable dipole moment without inducing the « exotic » S_A phases that often occur with CN or NO_2 endgroups. We report on the X-ray reflectivity from the surface of this compound and conclude that no bilayers are present in this case, despite the strongly polar character of the molecules. Consequences for molecular models of S_A phases will be discussed.

2. Experimental.

The experiments have been carried out at the Risø National Laboratory (Roskilde, Denmark) with a modified triple axis spectrometer as shown in figure 1. The liquid nature of the surface imposes the restriction on the scattering geometry that the sample remains horizontal under all circumstances. A similar set-up operated at a synchrotron source has been described elsewhere [5-7]. The X-ray source (A) is a

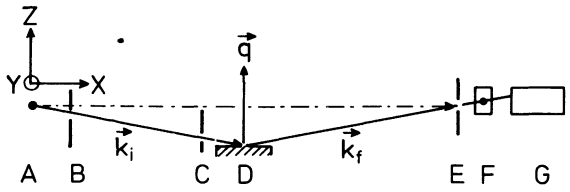

Fig. 1. — Side view of the spectrometer, with A : rotating anode X-ray source ; B, C : beam defining slits ; D : sample ; E : detector slit ; F : graphite analyser crystal ; G : detector. Horizontal dimensions : AB = 147 mm, AC = 717 mm, AD = 793 mm, ED = AD. Slit widths (vertical) : B : 0.2 mm, C : 0.05 mm, E : 2 mm ; horizontal 2 mm each. The picture is drawn for specular reflection ; the momentum transfer $\mathbf{q} \equiv \mathbf{k}_f - \mathbf{k}_i$ is then along the q_z axis.

Rigaku copper rotating anode operated at 50 kV and 180 mA. The natural divergence of the primary beam is used to select radiation incident on the horizontal sample surface (D) at an angle θ, by choosing the appropriate positions of the slits B and C. X-rays that are either specularly reflected from the surface or Bragg scattered from the smectic layers parallel to it, leave the surface at the same angle θ and pass through slit E onto the pyrolytic graphite analyzer crystal (F), which selects the K_α lines (λ = 1.54 Å). The slit and sample heights at B, C and D are controlled such that the beam always illuminates a fixed position of the sample. Slit E can be moved either vertically or horizontal ($/\!/y$) out of the specular reflection to monitor the background scattering from the bulk. A NaI scintillation counter (G) detects the scattered X-ray photons. Dimensions and slit sizes are indicated in the caption of figure 1. The resolution function in reciprocal space has widths (FWHM) $\Delta q_z \approx 5 \times 10^{-3}$ Å^{-1} in the vertical direction (q_z), $\Delta q_x \approx 2 \times 10^{-3}\, q_z$ in the horizontal in-plane direction (q_x) and $\Delta q_y \approx 0.02$ Å^{-1} in the horizontal out-of-plane direction (q_y). Note that Δq_x is proportional to q_z because the scattering is elastic ($|\mathbf{k}_f| = |\mathbf{k}_i|$).

The experiments were performed on the compound [8] :

4-isothiocyanatophenyl-4-
(trans-4-heptylcyclohexyl)-benzoate .

The structural formula and the phase transitions are :

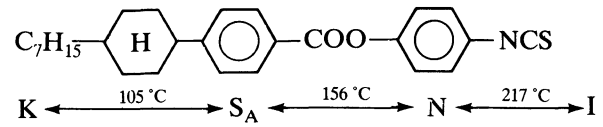

Samples are prepared as droplets put on a glass plate in the nematic or isotropic phase to flow out freely over an area of typically 10 cm^2, and then cooled down to the desired temperature. The glass plates are specially treated with either silane coatings or greasy fingers such that **n** is perpendicular to the glass plate as well as to the liquid crystal to air interface. The sample is placed in a two-stage oven with kapton windows ; the inner stage is electronically controlled with a stabilization better than 0.03 °C.

3. Results.

The X-ray reflectivity of the sample has been measured as a function of q_z with $q_x = q_y = 0$, for five temperatures around the N-S_A phase transition. The signal from the bulk, obtained with q_y offset to 0.02 Å^{-1}, was substracted to obtain the surface reflectivity $R(q_z)$. As an example, raw data of the scans with and without q_y offset are displayed in figure 2. The result should be compared with the reflectivity for radiation incident on a planar dielectric discontinuity as given by Fresnel's law, $R_F(q_z)$, which thus gives the background on which the structure of a realistic surface manifests itself [9]. As for X-rays the dielectric permittivity of the material is slightly smaller than 1 ($\varepsilon \approx 1 - 6 \times 10^{-6}$), Fresnel's law predicts total reflection for scattering angles θ smaller than $\theta_c \approx 0.15°$ (or $q_z < q_c \approx 0.02$ Å^{-1}) and a steep fall-off ~ q_z^{-4} above this angle.

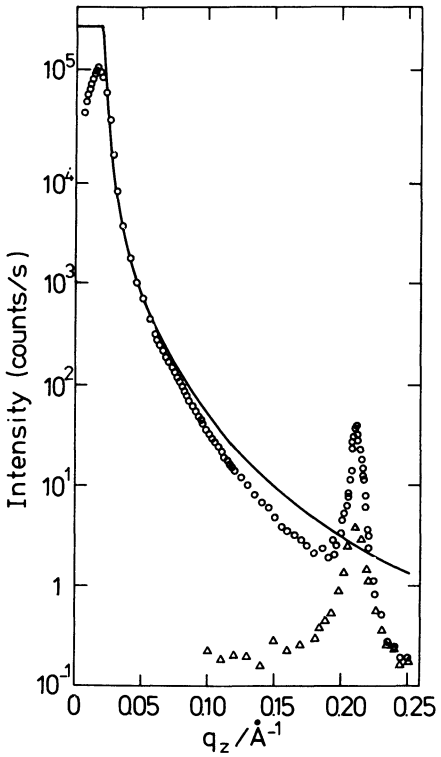

Fig. 2. — Intensity as a function of q_z, with $q_x = 0$ and $q_y = 0$ (circles) or $q_y = 0.02$ Å^{-1} (triangles : mean value for left and right offset) at T_{AN} + 1.5 °C. The surface signal is obtained as the difference between the two scans. The full line is the calculated Fresnel reflectivity multiplied with the intensity of the direct beam. At small q_z deviations occur as the beam shines over the edges of the sample.

The region of interest ($0.5° < \theta < 2.0°$) is well above θ_c. In this region, refraction away from the surface normal slightly decreases the wavevector transfer inside the material according to Snel's law : $q_{z,\text{in}} = (q^2_{z,\text{out}} - q_c^2)^{1/2}$. The reflectivity normalized to the Fresnel function, R/R_F, is shown as a function of the calculated wavevector inside the liquid crystal in figure 3. The peak at $q_z = q_0 \approx 0.22$ Å^{-1}, caused by pretransitional smectic layering which extends to a depth $\xi(T)$ below the surface, narrows and increases in intensity as the S_A phase is approached. It becomes resolution limited in the scan at the lowest temperature which is just below the critical temperature T_{AN}. At all temperatures, the intensity drops dramatically for $q_z > 1.1\, q_0$. In this region, there is no significant difference between the scans with and without offset in q_y. Consequently, only an upper boundary for R/R_F can be given here.

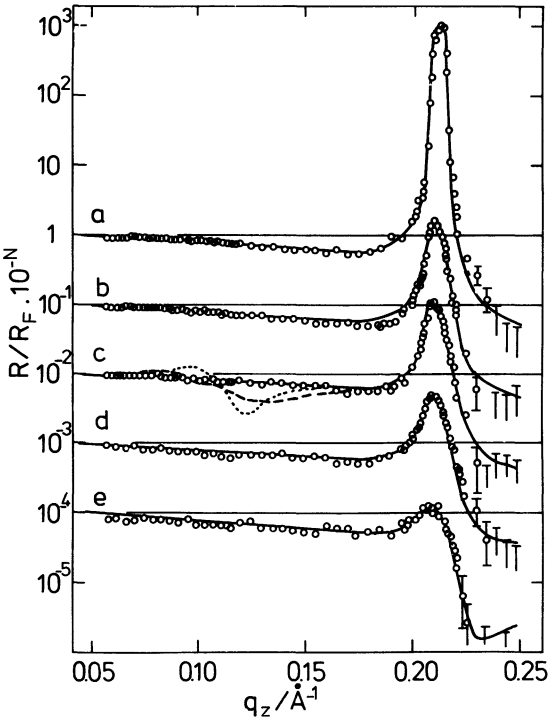

Fig. 3. — The measured reflectivity $R(q_z)$, relative to the calculated Fresnel reflectivity $R_F(q_z)$, as a function of the wavevector transfer q_z inside the liquid crystal. The temperatures $T - T_{AN}$ are : a) 0.5 °C, b) − 0.5 °C, c) − 1.5 °C, d) − 3.5 °C, e) − 6.5 °C. Data for each temperature have been displaced by one decade. The full lines represent the best least square fit to the model described in the text, convoluted with the resolution function. The broken lines in the curve for $T = T_{AN} + 1.5$ °C represent the hypothetical reflectivity with the addition of one (---) and two (...) full bilayers as explained in the text.

4. Discussion.

Starting point of any analysis of X-ray reflectivity data is the master formula, which relates the intensity of the reflected beam as a function of $\mathbf{q} = (0, 0, q)$ to the electron density profile $\rho(z)$ along the surface normal [9] :

$$\frac{R(q)}{R_F(q)} = \left|\bar{\rho}^{-1} \int (\mathrm{d}\rho/\mathrm{d}z) \exp(iqz)\, \mathrm{d}z\right|^2 \quad (1a)$$

$$= q^2 \left|\bar{\rho}^{-1} \int \rho(z) \exp(iqz)\, \mathrm{d}z\right|^2 \quad (1b)$$

$$\equiv q^2 |\phi(q)|^2 . \quad (1c)$$

Since the phase factor in the complex quantity $\phi(q)$ is lost we cannot obtain $\rho(z)$ directly from R/R_F. The alternative is to make an intelligent guess about the shape of $\rho(z)$ which, in general, contains a number of parameters which in turn can be fitted to the observed R/R_F curve. In order to maintain a connection to the molecular origin of the S_A layering, we take the electron density of a single molecule as the basis of our assumptions about $\rho(z)$. In addition, assumptions have to be made about the degree of layering at the surface and the way it decays into the bulk. If also bilayers are present, a similar set of assumptions is needed for the bilayering. The procedure for calculating R/R_F with these ingredients has been given in reference [3]. It turns out to be convenient to split the molecular electron density $\rho_m(\zeta)$ into its average value $\bar{\rho}$, the symmetric part $\rho_s(\zeta)$ and the antisymmetric part $\rho_a(\zeta)$, where ζ is a molecular coordinate along the z-axis with the origin in the middle of the molecule. The average $\bar{\rho}$ of all layers together naturally produces the Fresnel reflectivity. The monolayers, having equal numbers of molecules pointing up and down, produce a contribution to the electron density which is symmetric around $\zeta = 0$. The bilayering, on the other hand, depends on the difference between the numbers of molecules pointing up and down in each layer and the contribution to the electron density is antisymmetric around $\zeta = 0$. Hence the monolayering couples to $\rho_s(\zeta)$ and the bilayering to $\rho_a(\zeta)$:

$$\phi(q) = q^{-1} \exp\left(-\frac{1}{2} q^2 \sigma^2 - iqh\right) + [F_s(q)\, \varphi_s(q) + iF_a(q)\, \varphi_a(q)] \cdot \exp\left(-\frac{1}{2} q^2 \sigma_L^2\right) \quad (2)$$

(cf. Eq. (8) in Ref. [3]) where $F_s(q)$ and $F_a(q)$ are the Fourier transforms of $\rho_s(\zeta)$ and $\rho_a(\zeta)$. The complex functions $\varphi_s(q)$ and $\varphi_a(q)$ depend on the way the layering decays into the bulk. The Gaussian smearing parameters σ and σ_L are introduced to account for thermal roughness of the surface itself (capillary waves) and of the smectic layers, and h is the displacement of the actual surface above the first layer. This parameter is always needed in practice to allow for a « dirty » surface [3-7, 9].

The atomic coordinates, needed to construct $\rho_m(\zeta)$, are given in table I. The molecule is assumed

Table I. — *Atomic numbers Z and coordinates ζ of atoms and groups in different parts of the molecule :* a) *the alkyl chain,* b) *the cyclohexane ring,* c) *and* e) *the benzene rings,* d) *the bridge group between the benzene rings,* f) *the* NCS *polar group.*

Atom/ group	Z	ζ (Å)	Atom/ group	Z	ζ (Å)
a) CH_3	9	− 13.2	CH	7	1.5
CH_2	8	− 11.7	CH	7	2.1
CH_2	8	− 10.8	C	6	2.4
CH_2	8	− 9.3	d) C	6	3.9
CH_2	8	− 8.4	O	8	4.2
CH_2	8	− 6.9	O	8	4.9
CH_2	8	− 6.1	e) C	6	6.2
b) CH	7	− 4.6	CH	7	6.6
CH_2	8	− 3.9	CH	7	7.2
CH_2	8	− 3.9	CH	7	7.9
CH_2	8	− 2.4	CH	7	8.6
CH_2	8	− 2.4	C	6	8.9
CH	7	− 1.7	f) N	7	10.3
c) C	6	− 0.2	C	6	11.6
CH	7	0.1	S	16	13.2
CH	7	0.7			

to be in its most stretched configuration ; bond lengths and angles have been taken from space-filling molecular models. A coaxial spatial arrangement of the NCS group bound to the benzene ring has been used [10]. Analogous to other NCS compounds [11], the molecular length of 29.6 Å thus obtained (taking into account the extent of the electron clouds) approximates the layer thickness $d = 29.8$ Å. In making the fits to the experimental data, the first layer is assumed to have saturated smectic order. The layering vanishes into the bulk with an exponential decay curve characterized by a temperature dependent penetration depth $\xi(T)$. The absence of special features like peaks or dips near $q_0/2$ in the R/R_F curves suggests that there are no bilayers. Therefore, we first fitted the data to the model without bilayers, with ξ as the only temperature dependent parameter. The other parameters (q_0, h, σ, σ_L) were held constant for all temperatures. The parameter values as obtained from a nonlinear least-square fit are summarized in table II. These calculations include a convolution with the resolution function. The resultant reflectivity curves are given in figure 3. In addition, the hypothetical reflectivity curves were calculated for the cases that one or two fully developed bilayers are present at the surface. As can be seen in figure 3, this would result in a clearly observable deviation of R/R_F near $q_0/2$. Hence we conclude that the molecules have also at the surface a random up-down distribution.

Table II. — *Least-square fit values of the parameters in the model described in the text. A convolution with the resolution function of inverse width* (HWHM) 400 $Å^{-1}$ *has been included in the fitting procedure. The value of* ξ *labelled with an asterix is resolution limited.*

Parameter	Temperature $T - T_{AN}$ (°C)				
	− 0.5	0.5	1.5	3.5	6.5
ξ (Å)	15 000*	510	390	275	139
q_0	0.221 $Å^{-1}$	($2\pi/q_0 = 29.8$ Å)			
h	4.8 Å	independent of temperature			
σ	8.3 Å				
σ_L	7.8 Å				

The present observations are important for molecular models of the various types of S_A phase. In principle, one should expect at the interface between the air and the liquid crystal a tendency of the molecules to orient with their polar heads pointing away from the surface. This would lead to an oriented top layer, which may in turn orient the second layer in the opposite direction, and so on. Thus a number of S_{A2}-like bilayers can be formed. This is, in fact, exactly what has been observed in the S_{A1} and N phases at the surface of a compound with a terminal CN polar group [3]. In the present case, the dipole moment of the terminal group is only slightly less : 2.9 Debye for NCS against 4.0 Debye for CN [12]. The dipolar interaction energy of parallel neighbours in one layer is approximately $k_B T$ for NCS against $2 k_B T$ for CN. The fact that in the present case we do not observe such bilayers despite the still considerable dipole moment indicates that the « classical » S_A phase, though with polar molecules, differs qualitatively from the S_{A1} phase. In the former case, the molecular asymmetry is nullified by a random up-down distribution of the molecules and the resultant short-range structure is similar to that of symmetric molecules. In the latter case, the macroscopic symmetry is the same but the local structure is a bilayer one as in the S_{A2} phase. This leads to similar dielectric behaviour in the S_{A1} and S_{A2} phases [13]. The S_{A2} regions in the S_{A1} phase are assumed to be separated by « walls » as in the $S_{\tilde{A}}$ phase, in which the bilayers shift over a single molecular length, but with a random distribution of walls (see Fig. 4). This explains the diffuse scattering found near $q_0/2$ in the bulk [14]. These walls will be expelled from the surface, so that the underlying short-range bilayer structure reveals itself. In a « classical » S_A phase of polar molecules, the cooperative effect of the S_{A2}-like regions is absent. Orienting the top layer then means orienting

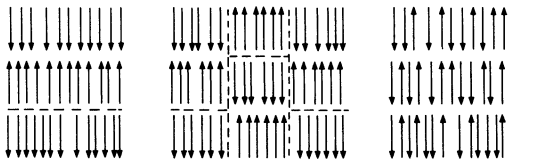

Fig. 4. — (a) S_{A2} : smectic layering with the orientation of the polar molecules alternating from layer to layer. (b) $S_{\tilde{A}}$: S_{A2}-like domains are separated by « walls » where the bilayer structure shifts over one molecular length. The regular pattern of walls becomes irregular in the S_{A1} phase as discussed in the text. (c) Classical S_A : smectic layering with random up-down order of the polar molecules. (For the sake of clarity the pictures have been drawn for perfect orientational and positional order.)

each molecule in this layer separately, which evidently costs too much energy to be compensated for by the more favourable orientation of the polar heads with respect to the surface.

5. Conclusion.

To our present state of understanding, two rather different types of molecular organization can lead to a monolayer smectic-A phase ($d \approx l$) with polar molecules. One is the S_{A1} phase with strong local up-down order of the dipoles, resembling the $S_{\tilde{A}}$ and S_{A2} phases. The other is the « classical » S_A phase, in which there is up-down disorder on a molecular scale so that the phase is effectively equivalent to one of symmetric molecules. The difference reveals itself more strikingly at smectic surfaces than it does in the bulk. An S_{A1} surface has been found to induce a number of bilayers, whereas at a classical S_A surface there are none. Since the dipoles involved are approximately equal (≈ 4 D for CN in S_{A1} and 3 D for NCS in classical S_A) the phase itself rather than the actual value of the dipoles must lie at the origin of the difference.

Acknowledgments.

The authors wish to thank Dr. R. Eidenschink (Merck, Darmstadt) for providing them with the substance, and Dr. J. Als-Nielsen for his support and stimulating discussions. The excellent research conditions provided by the Risø National Laboratory (Roskilde, Denmark) are gratefully acknowledged. This work forms part of the research program of the « Stichting voor Fundamenteel Onderzoek der Materie » (Foundation for Fundamental Research on Matter, FOM) and was made possible by financial support from the « Nederlandse Organisatie voor Zuiver Wetenschappelijk Onderzoek » (Netherlands Organisation for the Advancement of Pure Research, ZWO).

References

[1] For a review see : HARDOUIN, F., LEVELUT, A. M., ACHARD, M. F. and SIGAUD, G., *J. Chim. Phys.* **80** (1983) 53.

[2] (a) PROST, J. and BAROIS, P., *J. Chim. Phys.* **80** (1983) 65 ;
(b) BAROIS, P., PROST, J. and LUBENSKY, T. C., *J. Phys. France* **46** (1985) 391.

[3] GRAMSBERGEN, E. F., DE JEU, W. H. and ALS-NIELSEN, J., *J. Phys. France* **47** (1986) 711.

[4] OCKO, B. M., PERSHAN, P. S., SAFINYA, C. R. and CHIANG, L. Y., *Phys. Rev. A* **35** (1987) 1868.

[5] ALS-NIELSEN, J. and PERSHAN, P. S., *Nucl. Instrum. Methods* **208** (1983) 545.

[6] ALS-NIELSEN, J., CHRISTENSEN, F. and PERSHAN, P. S., *Phys. Rev. Lett.* **48** (1982) 1107.

[7] PERSHAN, P. S., BRASLAU, A., WEISS, A. H. and ALS-NIELSEN, J., *Phys. Rev. A* **35** (1987) 4800.

[8] EIDENSCHINK, R. and PAULUTH, D., unpublished results.

[9] ALS-NIELSEN, J., in *Handbook of Synchrotron Radiation*, Vol. 3, D. Moncton and G. Brown, eds. (North-Holland, Amsterdam) 1987.

[10] The deviation from collinearity is either zero or very small :
(a) ANTOS, K., MARTVON, A. and KRISTIÁN, P., *Collect. Czech. Chem. Commun.* **31** (1966) 3737.
(b) ULICKY, L., *Zb. Pr. Chemickotechnol. Fak. Syst.* (1969) 47.

[11] VAN DER VEEN, J., *J. Phys. Colloq. France* **37** (1976) C3-13.

[12] (a) SMITH, J. W., *Electric Dipole Moments* (Butterworths, London) 1955.
(b) MINKIN, V. I., OSIPOV, O. and ZHDANOV, Yu. A., *Dipole Moments in Organic Chemistry* (Plenum press, New York) 1970.

[13] (a) BENGUIGUI, L. and HARDOUIN, F., *J. Phys. France Lett.* **42** (1981) L-381 ;
(b) BENGUIGUI, L., HARDOUIN, F. and SIGAUD, G., *Mol. Cryst. Liq. Cryst.* **116** (1984) 35.

[14] GRAMSBERGEN, E. F., ALS-NIELSEN, J. and DE JEU, W. H., *Phys. Rev. A* (in press).